



Glacial–interglacial seawater isotope change near the Chilean Margin as reflected by $\delta^2\text{H}$ values of C_{37} alkenones

Katrin Hättig¹, Devika Varma¹, Stefan Schouten^{1,2}, and Marcel T. J. van der Meer¹

¹Department of Marine Microbiology and Biogeochemistry, NIOZ Royal Netherlands Institute for Sea Research, Texel, the Netherlands

²Department of Earth Sciences, Faculty of Geosciences, Utrecht University, Utrecht, the Netherlands

Correspondence: Katrin Hättig (katrin.haettig@nioz.nl)

Received: 17 May 2023 – Discussion started: 25 May 2023

Revised: 21 August 2023 – Accepted: 9 September 2023 – Published: 12 October 2023

Abstract. Stable hydrogen isotopic compositions of long-chain alkenones with 37 carbon atoms ($\delta^2\text{H}_{\text{C}_{37}}$) have been shown to reflect seawater salinity in culture and environmental studies, and this potential sea surface salinity proxy has been applied to several downcore records from different regions. However, previous studies were based solely on a single sediment core and often suggested unlikely large changes in salinity based on existing proxy calibrations. Here we present a new $\delta^2\text{H}_{\text{C}_{37}}$ record, in combination with oxygen isotopes of benthic foraminifera from the same samples, from a sediment core from the Chilean Margin (ODP Site 1235). The observed negative shift in $\delta^2\text{H}_{\text{C}_{37}}$ of 20‰ during the last deglaciation was identical to that of a previously published $\delta^2\text{H}_{\text{C}_{37}}$ record from the nearby, but deeper, ODP Site 1234, suggesting a regionally consistent shift in $\delta^2\text{H}_{\text{C}_{37}}$. This change translates into a negative hydrogen isotope shift in the surface seawater of ca. 14‰, similar to glacial–interglacial reconstructions based on other $\delta^2\text{H}_{\text{C}_{37}}$ records. The reconstructed bottom seawater oxygen isotope change based on benthic foraminifera during the last deglaciation is approximately -0.8‰ , in line with previous studies. When translated into hydrogen isotopes of bottom seawater using the modern open-ocean water line, this would suggest a negative change of ca. 5‰, smaller than the reconstructed surface seawater shift based on alkenones. The larger change in surface water isotopes suggests that it experienced more freshening during the Holocene than bottom waters, either due to increased freshwater input, reduced evaporation, or a combination of the two.

1 Introduction

The stable oxygen and hydrogen isotope composition of seawater ($\delta^{18}\text{O}_{\text{SW}}$ and $\delta^2\text{H}_{\text{SW}}$, respectively) reveal crucial information about (sea)water physicochemical properties, which improves our understanding of past global ocean current dynamics and changes therein. Several oceanographic factors can cause shifts in the isotopic composition of seawater: for example, the bottom seawater isotopic composition depends on the source area of the water and reflects the history of advection associated transport, mixing, upwelling, and downwelling of ocean currents (Rohling and Cooke, 1999). Regional factors affecting the surface seawater isotopic composition are the evaporation–precipitation balance, river water input, iceberg melting, and the local climate regime (Rohling and Cooke, 1999). On a more global level, land ice formation is an important process that affects oxygen and hydrogen isotopes of seawater, where during glacial periods large amounts of water with relatively low, more negative $\delta^{18}\text{O}$ and $\delta^2\text{H}$ values are stored as ice on land, increasing seawater $\delta^{18}\text{O}$ values (e.g. Schrag et al., 2002). Decreasing global ice volume during warmer interglacials releases this fresh, low-density water with relatively low $\delta^{18}\text{O}$ and $\delta^2\text{H}$ values into the surface ocean (Rohling and Bigg, 1998). Since both seawater isotopes and salinity increase as a result of evaporation and decrease as a result of precipitation or freshwater input, seawater isotopes and salinity are tightly coupled (Rohling, 2007; Craig, 1961; Craig and Gordon, 1965). Therefore, seawater isotopes are often reconstructed and used to infer past salinity changes (e.g. Lamy et al., 2002; Schrag et al., 2002; Rousselle et al., 2013).

There are several methods available to reconstruct the isotopic composition of seawater. The stable oxygen isotopic composition of foraminifera ($\delta^{18}\text{O}_{\text{foram}}$) is a function of $\delta^{18}\text{O}_{\text{SW}}$ and calcification temperature (Bemis et al., 1998; Epstein et al., 1953; Shackleton, 1974) with a minor effect of carbonate ion concentration (Spero et al., 1997). Temperature-corrected $\delta^{18}\text{O}_{\text{foram}}$ is thus assumed to reflect $\delta^{18}\text{O}_{\text{SW}}$, though with some uncertainty (Duplessy et al., 1991; Rostek et al., 1993). Generally, temperature corrections of $\delta^{18}\text{O}_{\text{foram}}$ to reconstruct $\delta^{18}\text{O}_{\text{SW}}$ are done based on temperature proxies derived from the same foraminifera, such as Mg/Ca (e.g. Billups and Schrag, 2002, 2003; Lear et al., 2000, 2004, 2015; Martin and Lea, 2002) or carbonate clumped isotopes (Δ_{47}) (e.g. Petersen and Schrag, 2015). In some cases, independent temperature proxies based on organic geochemical indices, such as U_{37}^{K} and TEX_{86} (Brassell et al., 1986; Prahl and Wakeham, 1987; Schouten et al., 2003), are used to correct for temperature (Rostek et al., 1993, 1997). Several studies based on $\delta^{18}\text{O}_{\text{foram}}$ records, $\delta^{18}\text{O}$ values of porewaters, and modelling estimate a negative global average change of 0.8‰–1.1‰ in the oxygen isotope ratio of seawater during the last deglaciation (e.g. Adkins and Schrag, 2001; Adkins et al., 2002; Duplessy et al., 2002; Oba and Murayama, 2004; Waelbroeck et al., 2002). Based on this, the salinity change is thought to be around 1–2 psu (Adkins et al., 2002; Broecker and Comer, 2002). Deriving salinity from local $\delta^{18}\text{O}_{\text{SW}}$ estimates, i.e. those corrected for global $\delta^{18}\text{O}_{\text{SW}}$ changes, requires knowledge of the regional relationship between $\delta^{18}\text{O}_{\text{SW}}$ and salinity (LeGrande and Schmidt, 2006; Rohling, 2007). However, it is uncertain whether this relationship is consistent through time.

The hydrogen isotopic composition of seawater is more difficult to reconstruct. Schrag et al. (2002) measured the hydrogen isotopic compositions of pore fluids in deep-sea sediments and showed a negative shift of 6‰–9‰ in the hydrogen isotopic composition of bottom seawater ($\delta^2\text{H}_{\text{BSW}}$) during the last glacial to interglacial transition. A potential proxy for reconstructing surface seawater ($\delta^2\text{H}_{\text{SSW}}$) is based on the combined hydrogen isotopic composition of long-chain alkenones with 37 carbon atoms and 2 and 3 double bonds ($\delta^2\text{H}_{\text{C}_{37}}$) derived from haptophyte algae. Culture studies show that the hydrogen isotopic fractionation of phototrophic organisms depends not only on the hydrogen isotopic composition of seawater but also on salinity (M’Boile et al., 2014; Sachs et al., 2016; Schouten et al., 2006; Weiss et al., 2017; Zhang et al., 2009; Zhang and Sachs, 2007). However, the response of $\delta^2\text{H}_{\text{C}_{37}}$ to salinity varies significantly between haptophyte species (M’Boile et al., 2014; Sachs et al., 2016; Schouten et al., 2006), as well as in different environmental settings where sometimes no impact of salinity on $\delta^2\text{H}_{\text{C}_{37}}$ is found (Gould et al., 2019; Häggi et al., 2015; Mitsunaga et al., 2022; Weiss et al., 2019a). These differences or absences in response of $\delta^2\text{H}$ to salinity make quantitatively constraining past salinity changes difficult. Down-core records show a decrease of 16‰–25‰ in $\delta^2\text{H}_{\text{C}_{37}}$ (when

corrected for ice volume 9‰–18‰) for the last deglaciation to the recent period depending on the site (Kasper et al., 2014; Pahnke et al., 2007; Petrick et al., 2015; Simon et al., 2015; Weiss et al., 2019b). Based on these results, Weiss et al. (2019b) reconstructed glacial–interglacial salinity changes of 5–19 psu based on multiple different $\delta^2\text{H}_{\text{C}_{37}}$ salinity calibrations. These reconstructed glacial–interglacial salinity changes are much larger than based on $\delta^{18}\text{O}$ and ice volume modelling (e.g. Oba and Murayama, 2004; Adkins et al., 2002). Therefore, Weiss et al. (2019b) concluded that either glacial–interglacial salinity changes are larger than previously assumed or the paleo-sensitivity of $\delta^2\text{H}_{\text{C}_{37}}$ to salinity changes was higher in the past than observed in modern-day environments and cultures.

A different approach is to correlate $\delta^2\text{H}_{\text{C}_{37}}$ with $\delta^2\text{H}_{\text{SSW}}$ rather than salinity. Gould et al. (2019) observed a statistically significant $\delta^2\text{H}_{\text{C}_{37}}$ – $\delta^2\text{H}_{\text{SSW}}$ relationship with open-ocean suspended particulate organic matter (SPOM), and Mitsunaga et al. (2022) showed a statistically identical relationship based on core top sediments. This suggests that in the natural environment, the effects of factors like salinity, species composition (e.g. Chivall et al., 2014; M’Boile et al., 2014), and light and nutrients (Sachs and Kawka, 2015; van der Meer et al., 2015) on stable hydrogen isotope fractionation during biosynthesis may be less important than the isotopic composition of seawater. This observation allows direct inference of $\delta^2\text{H}_{\text{SSW}}$ from $\delta^2\text{H}_{\text{C}_{37}}$ without any additional correction, though this approach has not been applied yet to reconstruct past $\delta^2\text{H}_{\text{SSW}}$. Mitsunaga et al. (2022) did suggest a “global” Last Glacial Maximum (LGM)–modern change of –12.7‰ in the hydrogen isotopic composition of alkenones based on the global $\delta^{18}\text{O}_{\text{SW}}$ shift, a waterline slope of 8, and their core top calibration. Similar to the process for $\delta^{18}\text{O}_{\text{SW}}$, reconstructed $\delta^2\text{H}_{\text{SSW}}$ can then be converted into salinity using modern-day correlations between surface $\delta^2\text{H}_{\text{SSW}}$ and salinity (LeGrande and Schmidt, 2006; Rohling, 2007).

Here, we generated a $\delta^2\text{H}_{\text{C}_{37}}$ and benthic $\delta^{18}\text{O}_{\text{foram}}$ record of ODP Site 1235 from the Chilean Margin (Fig. 1) and compared this with the previously published hydrogen isotope (Weiss et al., 2019b) and temperature records (de Bar et al., 2018) from nearby ODP Site 1234. Both cores are only ~12 km away from each other, albeit at a different water depths (489 m versus 1015 m) and are expected to record the same surface seawater signal (Mix et al., 2003). In contrast to Weiss et al. (2019b), we reconstructed $\delta^2\text{H}$ values of surface seawater and compared this to bottom seawater oxygen isotope values ($\delta^{18}\text{O}_{\text{BSW}}$) inferred from measured benthic foraminifera $\delta^{18}\text{O}$ values and used both to constrain relative salinity change during the deglaciation.

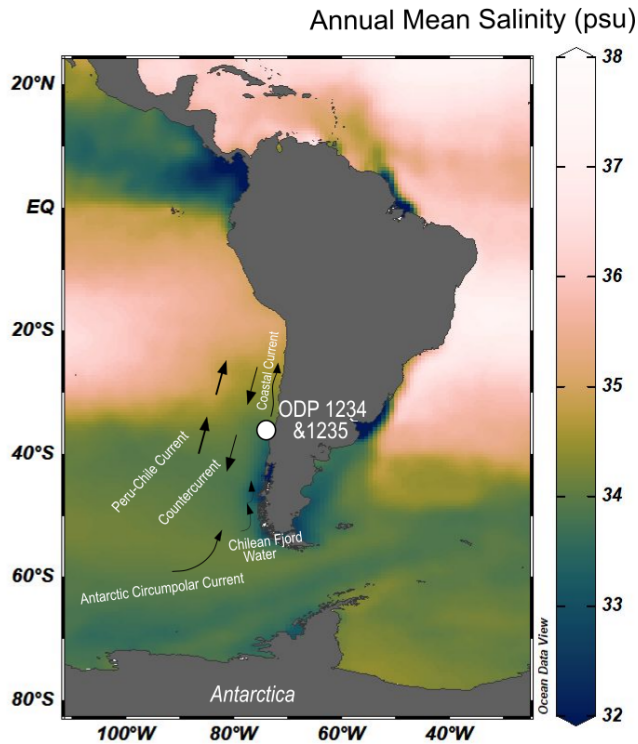


Figure 1. Map of sea surface salinity (data from Zweng et al., 2018) with a scientific colour map from Cramer (2023) showing the sediment core locations of the neighbouring core ODP Site 1234 and ODP Site 1235. The core location is influenced by three primary ocean currents: the Northward Peru–Chile Current and the Chilean Coastal Current, as well as the southward Peru–Chile Countercurrent. Those are fed by the Antarctic Circumpolar water mass, and Chilean Fjord waters can also enter from the southeast the system.

2 Material and methods

2.1 Geographic setting

The ODP Site 202–1235 was drilled at 36.16° S, 73.57° W at a relatively shallow water depth of 489 m (Fig. 1). The site is about 12 km away from the deeper neighbouring ODP Site 202–1234 (36.22° S, 73.68° W, water depth 1015 m) in the southeastern Pacific Ocean (Mix et al., 2003) (Fig. 1). These sites are located at the Chilean Margin, which is influenced by surface and deep-water currents that cause upwelling, stimulating local productivity (Bakun, 1989). The setting is dynamic, with southwesterly winds and freshwater runoff from the continent. The Antarctic Circumpolar Current (ACC) transports cold and saline water into the Peru–Chile Countercurrent (PCC) which could be mixed with fresher fjord water, with a lower $\delta^2\text{H}$ value, along the southern margin (Lamy et al., 2002; Strub et al., 1998; de Bar et al., 2018). The present-day annual mean sea surface salinity in the study area is 33.8 ± 0.2 psu (World Ocean Atlas 2018; 0.25° grid: Zweng et al., 2018).

2.2 Sampling and age model

Sediment samples of ODP Site 1235 were split into two sub-samples: approximately 6 g of wet sediment was used for foraminiferal oxygen isotope analysis ($\delta^{18}\text{O}_{\text{foram}}$), and approximately 10 g of wet sediment was used for organic proxy analysis, i.e. U_{37}^K , TEX_{86} (see Varma et al., 2023a, b) and $\delta^2\text{H}_{\text{C}_{37}}$ (this study). Samples were taken every 5–10 cm to cover a resolution of < 2 ka, and a total of 27 samples were analysed for hydrogen isotopes.

The age–depth models for ODP Site 1235 and the neighbouring ODP Site 1234 were both constructed with the statistical package Bacon (Blaauw and Christeny, 2011) using a Bayesian approach and are based on the radiocarbon ages of mixed benthic foraminifera (Muratli et al., 2010; this study, Table S1 in the Supplement) as outlined by Varma et al. (2023b). ODP Site 1234 has a mean sedimentation rate of 20 cm ka^{-1} , and ODP Site 1235 has a rate of 5 cm ka^{-1} .

2.3 Analysis of benthic foraminifera and long-chain alkenones

Stable oxygen isotopes were measured on the benthic foraminifera genus *Uvigerina* with an automated carbonate device (Kiel IV, Thermo Scientific) connected to a Thermo Finnigan MAT 253 dual-inlet isotope ratio mass spectrometer. The sample sizes were ca. 20 μg and contained two to five foraminifera shells (> 150 μm). Replicate analyses of $\delta^{18}\text{O}$ values of the same sample had a standard deviation of 0.016‰–0.2‰. NBS 19 limestone was used as the isotope calibration standard, and for drift detection and correction a second standard, NFHS 1, was used. For both standards the standard deviation is within 0.1‰ for $\delta^{18}\text{O}$. All carbonate isotope data are given in ‰ relative to VPDB (Vienna Pee Dee Belemnite). Calculated $\delta^{18}\text{O}$ seawater values are given in ‰ relative to VSMOW (Vienna Standard Mean Ocean Water) with the accepted conversion value of 0.27‰ (Hut, 1987; Pearson, 2012).

The sediment split for organic analysis was extracted as described by Varma et al. (2023b). Briefly, sediments were first freeze-dried and then extracted using a Dionex 350 Accelerated Solvent Extractor. The solvent from the total extract was first removed using a Turbovap and the last remaining water, if present, was removed using a small sodium sulfate column to obtain the total lipid extract (TLEs). The TLEs were separated into three fractions over a small aluminium oxide (Al_2O_3) column using hexane / dichloromethane 9 : 1 (v : v) to elute the apolar fraction, hexane / DCM 1 : 1 (v : v) to elute the ketone (alkenone) fraction, and dichloromethane / methanol 1 : 1 (v : v) to elute the polar fraction. The ketone fractions were used for compound-specific hydrogen isotope ratio measurements of alkenones after being measured using a gas chromatograph coupled to a flame ionisation detector (GC-FID) to determine the correct concentration and complexity of the

fraction. Hydrogen isotope ratios were measured in duplicate using a gas chromatograph coupled to a Thermo Delta V isotope ratio mass spectrometer via high-temperature conversion reactor (Isolink I) and Conflo IV. The GC was equipped with an RTX-200 with a 60 m column following Weiss et al. (2019b). We report the hydrogen isotope ratio, relative to VSMOW, of the individual alkenones $C_{37:3}$ and $C_{37:2}$ and the integrated C_{37} δ^2H ratios determined by manual peak integration of the combined $C_{37:3}$ and $C_{37:2}$ peaks (Van der Meer et al., 2013). The H3+ factor was measured daily before running samples and shifted in time never more than $0.5 \text{ ppm nA}^{-1} \text{ d}^{-1}$. The performance and stability of the instrument were monitored by measuring a standard containing 15 *n*-alkanes at different concentrations (Mix B from Arndt Schimmelmann, Indiana University), at the start of each day. Samples were only run when the average difference between the measured values for the Mix B standard and the certified values for this standard and their standard deviation were less than 5‰. With each sample, squalene and a C_{30} *n*-alkane were co-injected to monitor system performance. Their measured values of $-173 \pm 5 \text{‰}$ and $-78 \pm 4 \text{‰}$ fit well with their predetermined values of $-170 \pm 4 \text{‰}$ for squalene and $-79 \pm 5 \text{‰}$ for the C_{30} *n*-alkane.

2.4 Modern open-ocean isotopic composition of seawater

The relationship between $\delta^{18}O$ – δ^2H in the water–atmosphere environment can be described with the meteoric waterline (MWL) and is close to $\delta^2H = 8 \times \delta^{18}O + 10$ according to Craig (1961) and Craig and Gordon (1965). To describe the relationship in surface ocean waters and investigate the potential for palaeoceanographic applications, Rohling (2007) correlated measured $\delta^{18}O$ and δ^2H of sampled ocean waters (top 250 m). We updated the dataset of Rohling (2007) with data from the Waterisotope Database (2022) managed by Gabriel Bowen (University of Utah) and published data from Gould et al. (2019), Weiss et al. (2019a) and Srivastava et al. (2010) (Fig. S2). This extended seawater isotope dataset contains 1550 data points from all water depths, not limited to the top 250 or 300 m, from the open ocean:

$$\delta^2H_{\text{SW}} = 6.58(\pm 0.07) \times \delta^{18}O_{\text{SW}} - 0.12(\pm 0.03) \quad (1)$$

$$\left(R^2 = 0.82; \text{RMSE} = 3\text{‰} \right).$$

We will refer to this correlation as modern open-ocean water line (MOOWL). The relationship between the hydrogen isotopic composition of the surface seawater and the measured salinity in the modern open ocean is based on the top 300 m water depth, 424 data points are obtained from the extended seawater isotope dataset:

$$\delta^2H_{\text{SW}} = 3.53(\pm 0.10) \times S - 122.57(\pm 3.52) \quad (2)$$

$$\left(R^2 = 0.66; \text{RMSE} = 0.8 \text{ psu} \right).$$

Finally, the oxygen isotopic composition of the surface seawater (top 300 m) and the salinity were correlated based on 5602 data points:

$$\delta^{18}O_{\text{SW}} = 0.52(\pm 0.01) \times S - 18.02(\pm 0.18) \quad (3)$$

$$\left(R^2 = 0.64; \text{RMSE} = 0.8 \text{ psu} \right).$$

2.5 Calculation of past seawater isotopes

2.5.1 Bottom seawater

The oxygen isotopic composition of foraminifera depends mainly on the temperature of calcification (T) and isotope ratio of the water. McCrea (1950) published the first laboratory oxygen–isotope paleotemperature equation, which was subsequently revised and extended to different calcite polymorphs and foraminifera species (e.g. Bemis et al., 1998; Cramer et al., 2011; Epstein et al., 1953; Lynch-Stieglitz et al., 1999; Mulitza et al., 2003; O’Neil et al., 1969; Shackleton, 1974; Spero et al., 2003). The relationship can be described as the following, where d is the slope and c is the intercept:

$$T = c + d \times \left(\delta^{18}O_{\text{foram}} - \delta^{18}O_{\text{SW}} \right). \quad (4)$$

This relationship is used, in combination with temperature proxies, to reconstruct past $\delta^{18}O_{\text{SW}}$ values and subsequently obtain salinity estimations using the $\delta^{18}O_{\text{SW}}$ –salinity relationship (Lamy et al., 2002; Pearson, 2012; Tang and Stott, 1993; Ganssen et al., 2011). The most relevant paleotemperature equation for benthic foraminifera is currently from Lynch-Stieglitz et al. (1999), adjusted to VSMOW by Cramer et al. (2011), where the $\delta^{18}O$ –paleotemperature relationship is estimated with the in-field calibration of benthic foraminifera from the genera *Cibicidoides* and *Planulina* (Lynch-Stieglitz et al., 1999). *Uvigerina* genus $\delta^{18}O$ values are corrected to *Cibicidoides* and *Planulina* $\delta^{18}O$ values (e.g. Cramer et al., 2009, 2011). We adjusted the oxygen isotope ratios of *Uvigerina* in this study by 0.64‰ to fit with *Cibicidoides* and *Planulina* $\delta^{18}O$ values (i.e. Shackleton, 1974); these can be used for the $\delta^{18}O_{\text{BSW}}$ reconstruction. Important to note is that $\delta^{18}O_{\text{SW}}$ is always measured on the VSMOW scale, whereas calcite is standardised to VPDB. The accepted value to convert VPDB into VSMOW at the time of Eq. (5) (Cramer et al., 2011) is 0.27‰.

$$T = 16.1 - 4.76 \cdot \left(\delta^{18}O_{\text{foram}} - \left(\delta^{18}O_{\text{BSW}} - 0.27 \right) \right) \quad (5)$$

Rearranged to $\delta^{18}O_{\text{BSW}}$ this becomes the following equation:

$$\delta^{18}O_{\text{BSW}} = \frac{-16.1 + 4.76 \times \delta^{18}O_{\text{foram}} + T}{4.76} + 0.27. \quad (6)$$

2.5.2 Surface seawater

To estimate the $\delta^2\text{H}_{\text{SSW}}$ from the measured hydrogen isotopic composition of alkenones, we used the suspended organic matter calibration (SPOM) from Gould et al. (2019, reduced dataset):

$$\delta^2\text{H}_{\text{C}_{37}} = 1.48(\pm 0.4) \times \delta^2\text{H}_{\text{SSW}} - 199(\pm 3) \\ \left(R^2 = 0.2; \text{RSME} = 5.8\text{‰} \right). \quad (7)$$

The environmental $\delta^2\text{H}_{\text{C}_{37}} - \delta^2\text{H}_{\text{SSW}}$ calibration from Gould et al. (2019) is based on alkenones from mainly open-ocean Group III haptophytes living in the Atlantic and Pacific oceans, covering large environmental differences such as salinity, temperature, nutrient concentrations, and light intensity that in turn affect growth rate, for instance.

An alternative environmental calibration is the sediment core top study from Mitsunaga et al. (2022), where they extended and revised the data of Weiss et al. (2019a):

$$\delta^2\text{H}_{\text{C}_{37}} = 1.44(\pm 0.13) \times \delta^2\text{H}_{\text{SSW}} - 191.62(\pm 1.13) \\ \left(R^2 = 0.61; \text{RSME} = 7\text{‰} \right). \quad (8)$$

3 Results and discussion

3.1 Reconstruction of bottom seawater isotopes based on foraminifera

The $\delta^{18}\text{O}$ values of benthic *Uvigerina* in ODP core 1235 range between 4.15‰ and 2.27‰ (Fig. 1). Between 40 to 27 ka, the $\delta^{18}\text{O}_{\text{foram}}$ is relatively stable with values between 3.13‰ to 3.96‰, followed by a decrease towards a value of 2.27‰ at 25 ka. Between 25 and 20 ka, the $\delta^{18}\text{O}_{\text{foram}}$ is higher with values of 3.7‰–4.15‰ and rapidly shifts by 1.6‰ to values of 2.27‰ in the uppermost sample. This record is consistent with ODP Site 1234, showing a negative isotope shift from the LGM to 1 ka of ca. 1.7‰ in the $\delta^{18}\text{O}$ values of *Uvigerina* (de Bar et al., 2018).

To reconstruct $\delta^{18}\text{O}_{\text{BSW}}$, we need to reconstruct bottom water temperatures, which unfortunately, we were not able to do. To obtain some indications of temperature change, we used published sea surface temperature (SST) records from the same core. The organic SST proxy U_{37}^{K} measured in this core (from Varma et al., 2023a) indicates a temperature range of 11.9 to 16.9 °C, with relatively stable temperatures between 19 and 40 ka of ca. 13 °C and an increase of ca. 4 °C until 7 ka, after which it remained relatively stable (Fig. 1). The $\text{TEX}_{86}^{\text{H}}$ (from Varma et al., 2023a) reveals temperatures between 10.3 and 15.9 °C and a similar increase of 4 °C from 20 ka until ca. 1 ka. Thus, both proxies indicate a LGM-to-recent temperature change of ca. 4 °C, consistent with SST proxy records from ODP Site 1234, which also showed a temperature change of 4 °C from 20 ka until ca. 1 ka for both $\text{TEX}_{86}^{\text{H}}$ and U_{37}^{K} respectively (de Bar et al., 2018).

Adkins et al. (2002) and Adkins and Schrag (2001) suggested a similar bottom water temperature change of 4 °C for the Pacific, Southern, and Atlantic oceans, and thus we assume a similar temperature change for bottom water as reconstructed for surface water. Combined with the $\delta^{18}\text{O}$ values of *Uvigerina*, this translates to a negative $\delta^{18}\text{O}_{\text{BSW}}$ shift of $0.8 \pm 0.2\text{‰}$ (averaged values with standard deviation of ODP Site 1235 and 1234 and a temperature error of $\pm 1\text{ °C}$) from the LGM to 1 ka using Eq. (6). This $\delta^{18}\text{O}_{\text{BSW}}$ shift subsequently translates, using the modern open-ocean $\delta^{18}\text{O}_{\text{SW}} - \delta^2\text{H}_{\text{SW}}$ relationship described in Eq. (1) and considering the error of the slope, to a $\delta^2\text{H}_{\text{BSW}}$ shift of $-5.5 \pm 1.8\text{‰}$ for bottom waters. This is similar to the values reported Schrag et al. (2002), who measured oxygen and hydrogen isotopes of pore fluid from deep-sea sediments in the southern and northern Atlantic Ocean and observed a negative shift in $\Delta\delta^{18}\text{O}_{\text{BSW}}$ of 0.7‰–1.1‰ and $\Delta\delta^2\text{H}_{\text{BSW}}$ of 6‰–9‰ during the last deglaciation.

3.2 Reconstruction of surface seawater isotopes based on alkenones

The $\delta^2\text{H}_{\text{C}_{37}}$ values of ODP Site 1235 range between -193‰ and -169‰ (Fig. 2). Between 40 and 25 ka the stable isotope ratio is relatively stable at ca. -180‰ then increases to -169‰ and decreases again to -173‰ at the LGM (ca. 20 ka) and down to the more negative value of -193‰ in the most recent sample. This record compares well, both in trend and in absolute values, with that of the previously published $\delta^2\text{H}_{\text{C}_{37}}$ record of ODP Site 1234 (Weiss et al., 2019a; Fig. 2), confirming that the trends in $\delta^2\text{H}_{\text{C}_{37}}$ happened on a regional scale. If we calculate the overall shift from the LGM (21 ka) to the most recent sample, then both records show a shift in $\delta^2\text{H}_{\text{C}_{37}}$ of $-20 \pm 3\text{‰}$ (error indicates replicate analysis error). Published $\delta^2\text{H}_{\text{C}_{37}}$ records from Late Quaternary sediment cores (Kasper et al., 2014; Pahnke et al., 2007; Petrick et al., 2015; Simon et al., 2015; Weiss et al., 2019b) report $\delta^2\text{H}_{\text{C}_{37}}$ shifts that are very similar in magnitude (see overview in Table 1) and average $-20 \pm 3\text{‰}$ for the last deglaciation. This suggests that this shift in hydrogen isotopic composition of C_{37} alkenones is quite similar in magnitude for different oceans, despite the large differences in oceanographic settings.

Since Mix et al. (2003) observed the dominance of the open-ocean species *E. huxleyi* coccoliths of ODP Site 1234 and Hagino and Okada (2004, 2006) and Menschel et al. (2016) showed that the dominant alkenone producer on the western coast of South America is the Group III haptophyte *E. huxleyi*, it is most likely that alkenones in both cores reflect an open-ocean Group III haptophyte signal. We can therefore apply the SPOM calibration of Gould et al. (2019) (Eq. 7) to estimate the hydrogen isotopic composition of the seawater from the $\delta^2\text{H}_{\text{C}_{37}}$. The resulting record (Fig. 2) shows a $\delta^2\text{H}_{\text{SSW}}$ value of ca. 4‰ for the uppermost sample and ca. 18‰ for the LGM for ODP 1235 (Table 1). Con-

Table 1. Comparison of the seawater isotope changes between the Last Glacial Maximum (21 ka) to the recent period for different sediment cores. Calculated hydrogen isotopic composition of seawater is based on SPOM calibration (Gould et al., 2019) and sediment core top calibration (Mitsunaga et al., 2022). Oxygen isotopes of the bottom seawater are calculated with Cramer et al. (2011) and a temperature change estimate of 4 °C. For Petrick et al. (2015), a bottom water temperature change of 2 °C is estimated based on the SST data from that record.

Core	Location	Source	Recent			LGM			Difference LGM–Recent				
			Age (ka)	$\delta^2\text{H}_{\text{C}_{37}}$ (‰)	$\delta^2\text{H}_{\text{SSW}}$ (‰) SPOM	$\delta^2\text{H}_{\text{SSW}}$ (‰) Core top	Age (ka)	$\delta^2\text{H}_{\text{C}_{37}}$ (‰)	$\delta^2\text{H}_{\text{SSW}}$ (‰) SPOM	$\delta^2\text{H}_{\text{SSW}}$ (‰) Core top	$\Delta\delta^2\text{H}_{\text{C}_{37}}$ (‰)	$\Delta\delta^2\text{H}_{\text{SSW}}$ (‰) SPOM	$\Delta\delta^2\text{H}_{\text{SSW}}$ (‰) Core top
JPC32	Panama Basin	Pahnke et al. (2007)	0.3	−221	−15	−20	21.1	−198	1	−4	−23	−16	−16
MD02-2594	Southern South Africa	Kasper et al. (2014)	3.5	−192	5	0	21.1	−173	18	13	−19	−13	−13
164PE304-80	Mozambique channel	Kasper et al. (2015)	0.8	−189	7	2	21.3	−196	2	−3	7	5	6
ODP 1087	Southwestern Africa	Petrick et al. (2015)	2.7	−205	−4	−9	23.1	−180	13	8	−25	−17	−17
CD154 10-06P	Southeast Africa	Simon et al. (2015)	2	−195	3	−2	20.1	−179	14	9	−16	−11	−11
ODP 1234	Chilean Margin	Weiss et al. (2019b)	1	−195	3	−2	20.1	−176	16	11	−19	−13	−13
ODP 1235	Chilean Margin	This study	1.1	−193	4	−1	20.6	−173	18	13	−20	−14	−14
			Age (ka)	$\delta^{18}\text{O}_{\text{foram}}$ (‰)			Age (ka)	$\delta^{18}\text{O}_{\text{foram}}$ (‰)			$\Delta\delta^{18}\text{O}_{\text{foram}}$ (‰)	$\Delta\delta^{18}\text{O}_{\text{SSW}}$ (‰)	$\Delta\delta^2\text{H}_{\text{BSW}}$ (‰)
ODP 1234	Chilean Margin	Weiss et al. (2019b)	0.78	3.3			20.1	5			−1.7	−0.9	−6.2
ODP 1235	Chilean Margin	This study	0.9	2.3			20.56	3.8			−1.5	−0.7	−4.8
ODP 1087	Southwest Africa	Petrick et al. (2015)	1.6	2.7			21.1	4			−1.3	−0.9	−6.2
LRO4 stack	Global	Lisiecki and Raymo (2005)	0	3.2			20	5			−1.8	−1	−6.8

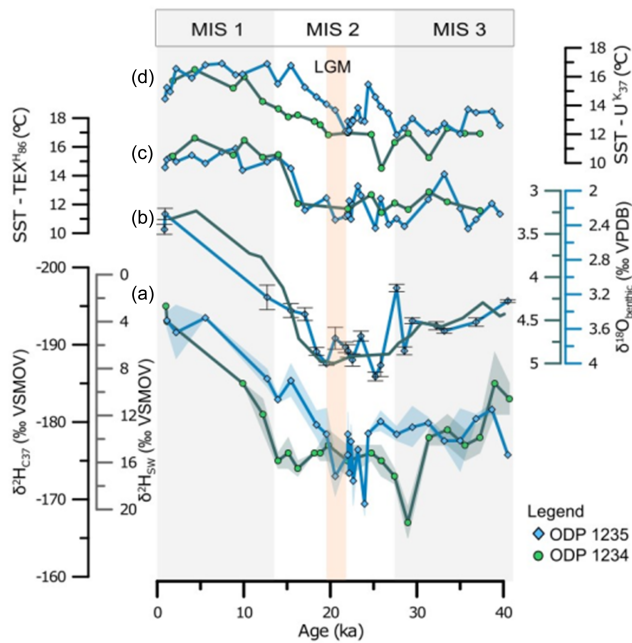


Figure 2. (a) Hydrogen isotope records of C_{37} alkenones of ODP Site 1235 (blue diamonds) and neighbouring ODP Site 1234 (Weiss et al., 2019) (green circles), which are both from the Chilean Margin. The shading represents the standard deviation of duplicate isotope measurements. Also shown are δ^2H values of surface seawater calculated using Gould et al. (2019). (b) The $\delta^{18}O$ of *Uvigerina* from ODP Site 1235 is in blue with diamonds, and error bars indicate standard deviation. The green line shows the five-point-average $\delta^{18}O$ of benthic foraminifera from ODP Site 1234 (from de Bar et al., 2018). Published organic proxy reconstructions are shown in (c) with TEX_{86}^H and (d) U_{37}^K index. SST data from ODP Site 1234 are from de Bar et al. (2018), and data from ODP Site 1235 are from Varma et al. (2023a).

version of the shift in $\delta^2H_{C_{37}}$ of $-20 \pm 3\text{‰}$ into $\Delta\delta^2H_{SSW}$, using the calibration of Gould et al. (2019) and considering the error in the slope of that calibration, results in a shift of $-14 \pm 4\text{‰}$ from the LGM to the most recent sample. Application of the core top calibration from Mitsunaga et al. (2022) (Eq. 8) gives an identical change of $-14 \pm 3\text{‰}$.

3.3 Comparison of seawater isotopes and paleo-salinity implications

The reconstructed $\Delta\delta^2H_{SSW}$ of ca. -14‰ from C_{37} alkenones is higher than that inferred from the benthic foraminifera isotopes (ca. -5‰) and measured in pore fluids (Schrag et al., 2002), implying that the isotopic composition of the sea surface water experienced a larger change during the last deglaciation compared to the bottom water isotope composition at the Chilean Margin. Potentially, we underestimated the change in the latter due to a lack of reconstructed bottom water temperatures. However, sensitivity analysis shows that even with much smaller bottom wa-

ter temperature changes than used here, the magnitude of δ^2H_{BSW} change will still be lower than that of δ^2H_{SSW} . For example, in the unlikely scenario that bottom water temperatures have remained constant, the maximum change of $\Delta\delta^{18}O_{BSW}$ is still only $-1.6 \pm 0.2\text{‰}$ or $-10.6 \pm 2\text{‰}$ of $\Delta\delta^2H_{BSW}$. Thus, it seems likely that at the Chilean Margin the glacial–interglacial change in surface water isotopes was larger than that of bottom water isotopes. The large regional change in δ^2H_{SSW} could be due to changes in local climate resulting in increased precipitation and/or decreased evaporation or increased freshwater runoff, for instance. Both cores, ODP Site 1235 and ODP Site 1234, are located within the Chile–Peru upwelling system and near two major river mouths, Río Biobío and Río Itata, both draining large basins (Muratli et al., 2010). However, de Bar et al. (2018) observed no major change in the contribution of terrestrially derived biomarker concentrations or proxies for river-transported material like the BIT index (Hopmans et al., 2016) and the C_{32} 1,15-diol index (de Bar et al., 2016; Lat-taud et al., 2017a, b).

To reconstruct salinity change we applied the modern open-ocean δ^2H_{SW} –salinity and $\delta^{18}O_{SW}$ –salinity relationships (Eqs. 2 and 3; based on data from 0–300 m depth). The bottom water $\Delta\delta^{18}O_{BSW}$ based on measured benthic foraminifera $\delta^{18}O$ values, translated using Eq. (3) and considering the error in the slope, corresponded to a change in bottom water salinity of 1 ± 0.2 psu and are in line with earlier estimations based on oxygen isotopes and sea level reconstructions (e.g. Adkins et al., 2002; Duplessy et al., 2002; Oba and Murayama, 2004; Waelbroeck et al., 2002). The $\Delta\delta^2H_{SSW}$ of ca. -14‰ , based on $\delta^2H_{C_{37}}$, translates using Eq. (2) and considering the error in the slope, to a regional salinity change of ca. 3 ± 1 psu, a larger reconstructed change than for bottom waters but similar to the estimate of Lamy et al. (2002), who reconstructed a sea surface paleo-salinity shift from 36 to 33 psu during the last 8 ka based on $\delta^{18}O$ of planktic foraminifera for the southern Chilean Margin core ODP 1233. The observed freshening in the surface waters relative to bottom waters may be due to a stronger input in relatively low-salinity waters from the Southern Ocean (ACC/PCC) and/or more transport of low-salinity Chilean Fjord Water (CFW) that, as a result of higher temperatures and intensifying continental meltwater input, resulted in even lower salinity surface water at the study site.

3.4 Global distribution of hydrogen isotope changes during the last deglaciation

To examine the global distribution of hydrogen isotopes during the last deglaciation we compare the two Chilean Margin records to published global alkenone hydrogen isotope records (Table 1). These comprise five low- to mid-latitude records of which four show a negative glacial–interglacial shift, while the record from the Mozambique Channel of Kasper et al. (2015) reflects a positive change. The latter may

be due to the close location to the river mouth, with varying freshwater input during the last 20 kyr, and therefore this record is not further considered here. If we calculate $\delta^2\text{H}_{\text{SSW}}$ from the remaining four published $\delta^2\text{H}_{\text{C}_{37}}$ records and compare this to our record, we find a remarkably similar negative shift from the LGM to the recent period in the $\delta^2\text{H}_{\text{SSW}}$ between 11‰–17‰ for different parts of the globe (Table 1), suggesting there might be a global aspect to this relatively large negative glacial–interglacial shift in surface seawater hydrogen isotope composition. This shift is larger than the shift inferred for bottom seawaters (e.g. Schrag et al., 2002).

There could be several reasons for this globally observed similar change in surface water hydrogen isotopic composition. For example, increasing average global temperatures during the deglaciation could have intensified the hydrological cycle, leading to high precipitation rates and runoff (including meltwater) in many places across the globe, at least around South America and southern Africa where most records originate from. This increased freshening of surface waters may have led to an additional depletion in ^2H compared to those of bottom waters. Another reason could be a change in the global waterline between the glacial and interglacial, where the slope of the $\delta^2\text{H}$ – $\delta^{18}\text{O}$ relationship changed for the surface waters. Rohling (2007) showed, for example, that the $\delta^{18}\text{O}$ – $\delta^2\text{H}$ relationship of the evaporative Mediterranean is significantly different from that of the modern open ocean, and Putman et al. (2019) suggested that hydroclimate processes are important controls on the slope and intercept of local meteoric water lines. Surface waters may be more sensitive to changes in the $\delta^{18}\text{O}$ – $\delta^2\text{H}$ relationship due to their direct atmosphere connection in contrast to bottom waters.

To verify these assumptions, further application of $\delta^2\text{H}_{\text{C}_{37}}$ analyses of sediment cores at different open-ocean locations and combined $\delta^{18}\text{O}$ foraminifera analyses or pore fluid oxygen and hydrogen isotope reconstructions (Schrag et al., 2002) are needed to study the past open-ocean waterline. Extending our understanding of the (past) relationship of seawater isotopes and salinity could help us to understand and reconstruct ocean current and ocean mixing processes.

4 Conclusion

The ODP 1235 sediment record shows a large shift in $\delta^2\text{H}_{\text{C}_{37}}$ during the last deglaciation at the Chilean Margin similar to the observation reported in Weiss et al. (2019b) for nearby core ODP Site 1234, demonstrating that the shift is regionally consistent. The hydrogen isotope ratios of alkenones are thus a reproducible paleo-proxy for relative changes in $\delta^2\text{H}_{\text{SSW}}$ and likely suggests changes in the salinity of the surface water. The reconstructed glacial–interglacial change in the hydrogen isotopic composition of surface seawater is ca. –14‰, using either the Gould et al. (2019) or Mitsunaga et al. (2022) calibration. In contrast, the change in hydrogen

isotopic composition of the bottom seawater reconstructed with the oxygen isotopic signature of benthic foraminifera was only ca. –5‰. Published C_{37} alkenone records from other oceans reveal a similarly large $\delta^2\text{H}_{\text{SSW}}$ change. More freshening of the surface waters or a change in the slope of the modern $\delta^{18}\text{O}$ – $\delta^2\text{H}$ open-ocean waterline possibly took place. Further application of $\delta^2\text{H}_{\text{C}_{37}}$ analyses combined with $\delta^{18}\text{O}$ foraminifera analyses or pore fluid oxygen and hydrogen isotope reconstructions may improve our understanding of the past ocean seawater isotopic composition and salinity changes between surface and bottom water.

Data availability. This study contains a Supplement. Supplement file 1 includes the age model and additional figures of the modern open-ocean salinity and isotope dataset used and cited in this study. Supplement file 2 contains the analysed isotope data of ODP Site 1235. The age model, sea surface temperature, and isotope dataset are archived at PANGAEA (<https://doi.org/10.1594/PANGAEA.957070>, Hättig et al., 2023a; <https://doi.org/10.1594/PANGAEA.958880>, Hättig et al., 2023b; <https://doi.org/10.1594/PANGAEA.957090>, Varma et al., 2023a).

Sample availability. All processed sediment samples are stored at NIOZ, i.e. TLE, apolar, ketone, polar fractions of ODP Site 1234 and ODP Site 1235 and sieved material of ODP Site 1235.

Supplement. The supplement related to this article is available online at: <https://doi.org/10.5194/cp-19-1919-2023-supplement>.

Author contributions. All four (co-)authors collectively contributed to the conceptualisation of this study. DV and KH ordered samples from IODP and made sample splits for different analysis. DV prepared apolar, ketone, and polar fractions and analysed alkenone and GDGTs for sea surface temperature. KH analysed the hydrogen isotopic composition of alkenones and performed the inorganic sample preparation, analysis, and age model computation.

Visualisation of research results and original draft preparation was done by KH. SSc, MTJvdM, and DV reviewed and edited the original draft.

Competing interests. The contact author has declared that none of the authors has any competing interests.

Disclaimer. Publisher's note: Copernicus Publications remains neutral with regard to jurisdictional claims in published maps and institutional affiliations.

Acknowledgements. We thank Michelle Penkrot from IODP Gulf Coast Repository for providing samples of ODP Site 1235. Jort

Ossebaar, Ronald van Bommel, and Piet van Gaever are thanked for analytical support.

Financial support. This work was carried out under the umbrella of the Netherlands Earth System Science Centre (NESSC). This project has received funding from the European Union’s Horizon 2020 research and innovation programme under the Marie Skłodowska-Curie Action (grant agreement no. 847504).

Review statement. This paper was edited by Erin McClymont and reviewed by two anonymous referees.

References

- Adkins, J. and Schrag, D. P.: Pore fluid constraints on deep ocean temperature and salinity during the last glacial maximum, *American Geophysical Union*, 28, 771–774, 2001.
- Adkins, J. F., McIntyre, K., and Schrag, D. P.: The salinity, temperature, and $\delta^{18}\text{O}$ of the glacial deep ocean, *Science*, 298, 1769–1773, <https://doi.org/10.1126/science.1076252>, 2002.
- Bakun, A.: Global Climate Change and Intensification of Coastal Ocean Upwelling, *Science*, 247, 198–201, 1989.
- Bemis, B. E., Spero, H. J., Bijma, J., and Lea, D. W.: Reevaluation of the oxygen isotopic composition of planktonic foraminifera: Experimental results and revised paleotemperature equations, *Paleoceanography*, 13, 150–160, <https://doi.org/10.1029/98PA00070>, 1998.
- Billups, K. and Schrag, D. P.: Paleotemperatures and ice volume of the past 27 Myr revisited with paired Mg/Ca and $^{18}\text{O}/^{16}\text{O}$ measurements on benthic foraminifera, *Paleoceanography*, 17, 3–13–11, <https://doi.org/10.1029/2000pa000567>, 2002.
- Billups, K. and Schrag, D. P.: Application of benthic foraminiferal Mg/Ca ratios to questions of Cenozoic climate change, *Earth Planet. Sc. Lett.*, 209, 181–195, [https://doi.org/10.1016/S0012-821X\(03\)00067-0](https://doi.org/10.1016/S0012-821X(03)00067-0), 2003.
- Blaauw, M. and Christeny, J. A.: Flexible paleoclimate age-depth models using an autoregressive gamma process, *Bayesian Anal.*, 6, 457–474, <https://doi.org/10.1214/11-BA618>, 2011.
- Brassell, S., Eglinton, G., and Marlowe, I.: Molecular stratigraphy: a new tool for climatic assessment, *Nature*, 129–133, <https://doi.org/10.1038/320129a0>, 1986.
- Broecker, W. S. and Comer, G.: The Glacial World according to Wally, Eldigio Press, https://www.ldeo.columbia.edu/~broecker/Home_files/GlacialWorld.pdf (last access: 11 October 2023), 2002.
- Chivall, D., M’Boule, D., Sinke-Schoen, D., Sinninghe Damsté, J. S., Schouten, S., and van der Meer, M. T. J.: The effects of growth phase and salinity on the hydrogen isotopic composition of alkenones produced by coastal haptophyte algae, *Geochim. Cosmochim. Ac.*, 140, 381–390, <https://doi.org/10.1016/j.gca.2014.05.043>, 2014.
- Craig, H.: Isotopic Variations in Meteoric Waters, *Science*, 133, 1702–1703, <https://doi.org/10.1126/science.133.3465.1702>, 1961.
- Craig, H. and Gordon, L. I.: Deuterium and oxygen 18 variations in the ocean and the marine atmosphere, in: *Stable Isotopes in Oceanographic Studies and Paleotemperatures*, edited by: Tongiorgi, E., Cons. Naz. di Rech., Spoleto, Italy, 9–130, 1965.
- Cramer, B. S., Toggweiler, J. R., Wright, J. D., Katz, M. E., and Miller, K. G.: Ocean overturning since the Late Cretaceous: Inferences from a new benthic foraminiferal isotope compilation, *Paleoceanography*, 24, 1–14, <https://doi.org/10.1029/2008PA001683>, 2009.
- Cramer, B. S., Miller, K. G., Barrett, P. J., and Wright, J. D.: Late Cretaceous–Neogene trends in deep ocean temperature and continental ice volume: Reconciling records of benthic foraminiferal geochemistry ($\delta^{18}\text{O}$ and Mg/Ca) with sea level history, *J. Geophys. Res.–Oceans*, 116, C12023, <https://doi.org/10.1029/2011JC007255>, 2011.
- Cramer, F.: Scientific colour maps (8.0.0), Zenodo [data set], <https://doi.org/10.5281/zenodo.5501399>, 2023.
- de Bar, M. W., Dorhout, D. J. C., Hopmans, E. C., Rampen, S. W., Sinninghe Damsté, J. S., and Schouten, S.: Constraints on the application of long chain diol proxies in the Iberian Atlantic margin, *Org. Geochem.*, 101, 184–195, <https://doi.org/10.1016/j.orggeochem.2016.09.005>, 2016.
- de Bar, M. W., Stolwijk, D. J., McManus, J. F., Sinninghe Damsté, J. S., and Schouten, S.: A Late Quaternary climate record based on long-chain diol proxies from the Chilean margin, *Clim. Past*, 14, 1783–1803, <https://doi.org/10.5194/cp-14-1783-2018>, 2018.
- Duplessy, J. C., Labeyrie, L., Juillet-Leclerc, A., Maitre, F., Duprat, J., and Sarthein, M.: Surface salinity reconstruction of the North Atlantic Ocean during the Last Glacial maximum, *Oceanol. Acta*, 14, 311–324, 1991.
- Duplessy, J. C., Labeyrie, L., and Waelbroeck, C.: Constraints on the ocean oxygen isotopic enrichment between the last glacial maximum and the holocene: Paleoceanographic implications, *Quaternary Sci. Rev.*, 21, 315–330, [https://doi.org/10.1016/S0277-3791\(01\)00107-X](https://doi.org/10.1016/S0277-3791(01)00107-X), 2002.
- Epstein, S., Buchsbaum, R., Lowenstam, H. A., and Urey, H. C.: Revised Carbonate–Water Isotopic Temperature Scale, *GSA Bull.*, 64, 1315–1326, [https://doi.org/10.1130/0016-7606\(1953\)64\[1315:RCITS\]2.0.CO;2](https://doi.org/10.1130/0016-7606(1953)64[1315:RCITS]2.0.CO;2), 1953.
- Ganssen, G. M., Peeters, F. J. C., Metcalfe, B., Anand, P., Jung, S. J. A., Kroon, D., and Brummer, G. J. A.: Quantifying sea surface temperature ranges of the Arabian Sea for the past 20 000 years, *Clim. Past*, 7, 1337–1349, <https://doi.org/10.5194/cp-7-1337-2011>, 2011.
- Gould, J., Kienast, M., Dowd, M., and Schefuß, E.: An open-ocean assessment of alkenone δD as a paleosalinity proxy, *Geochim. Cosmochim. Ac.*, 246, 478–497, <https://doi.org/10.1016/j.gca.2018.12.004>, 2019.
- Häggi, C., Chiessi, C. M., and Schefuß, E.: Testing the D/H ratio of alkenones and palmitic acid as salinity proxies in the Amazon Plume, *Biogeosciences*, 12, 7239–7249, <https://doi.org/10.5194/bg-12-7239-2015>, 2015.
- Hagino, K. and Okada, H.: Floral response of coccolithophores to progressive oligotrophication in the South Equatorial Current, Pacific Ocean, in: *Global Environmental Change in the Ocean and on Land*, edited by: Shiyomi, M., Kawahata, H., Koizumi, H., Tsuda, A., and Awaya, Y., TERRAPUB, 121–132, 2004.
- Hagino, K. and Okada, H.: Intra- and infra-specific morphological variation in selected coccolithophore species in the equatorial and subequatorial Pacific Ocean, *Mar. Micropaleontol.*, 58, 184–206, <https://doi.org/10.1016/j.marmicro.2005.11.001>, 2006.

- Hättig, K., Varma, D., van der Meer, M. T. J., Reichert, G.-J., and Schouten, S.: Age model for ODP Leg 202 Site 1235 and Site 1234, PANGAEA [data set], <https://doi.org/10.1594/PANGAEA.957070>, 2023a.
- Hättig, K., Varma, D., van der Meer, M. T. J., and Schouten, S.: Hydrogen isotopic composition of alkenones and oxygen isotopes of benthic foraminifera from ODP Site 202-1235. PANGAEA [data set], <https://doi.org/10.1594/PANGAEA.958880>, 2023b.
- Hopmans, E. C., Schouten, S., and Sinninghe Damsté, J. S.: The effect of improved chromatography on GDGT-based palaeoproxies, *Org. Geochem.*, 93, 1–6, <https://doi.org/10.1016/j.orggeochem.2015.12.006>, 2016.
- Hut, G.: Consultants' group meeting on stable isotope reference samples for geochemical and hydrological investigations, Int. At. Energy Agency, 49 pp. https://inis.iaea.org/search/search.aspx?orig_q=RN:18075746 (last access: 10 October 2023), 1987.
- Kasper, S., van der Meer, M. T. J., Mets, A., Zahn, R., Sinninghe Damsté, J. S., and Schouten, S.: Salinity changes in the Agulhas leakage area recorded by stable hydrogen isotopes of C₃₇ alkenones during Termination I and II, *Clim. Past*, 10, 251–260, <https://doi.org/10.5194/cp-10-251-2014>, 2014.
- Kasper, S., van der Meer, M. T. J., Castañeda, I. S., Tjallingii, R., Brummer, G.-J. A., Sinninghe Damsté, J. S., and Schouten, S.: Testing the alkenone D/H ratio as a paleo indicator of sea surface salinity in a coastal ocean margin (Mozambique Channel), *Org. Geochem.*, 78, 62–68, <https://doi.org/10.1016/j.orggeochem.2014.10.011>, 2015.
- Lamy, F., Rühlemann, C., Hebbeln, D., and Wefer, G.: High- and low-latitude climate control on the position of the southern Peru-Chile Current during the Holocene, *Paleoceanography*, 17, 16–16-10, <https://doi.org/10.1029/2001pa000727>, 2002.
- Lattaud, J., Dorhout, D., Schulz, H., Castañeda, I. S., Schefuß, E., Sinninghe Damsté, J. S., and Schouten, S.: The C₃₂ alkane-1,15-diol as a proxy of late Quaternary riverine input in coastal margins, *Clim. Past*, 13, 1049–1061, <https://doi.org/10.5194/cp-13-1049-2017>, 2017a.
- Lattaud, J., Kim, J.-H., De Jonge, C., Zell, C., Sinninghe Damsté, J. S., and Schouten, S.: The C₃₂ alkane-1,15-diol as a tracer for riverine input in coastal seas, *Geochim. Cosmochim. Acta*, 202, 146–158, 2017b.
- Lear, C. H., Wilson, P. A., Shackleton, N. J., and Elderfield, H.: Palaeotemperature and ocean chemistry records for the Palaeogene from Mg/Ca and Sr/Ca in benthic foraminiferal calcite, *GFF*, 122, 93, <https://doi.org/10.1080/11035890001221093>, 2000.
- Lear, C. H., Rosenthal, Y., Coxall, H. K., and Wilson, P. A.: Late Eocene to early Miocene ice sheet dynamics and the global carbon cycle, *Paleoceanography*, 19, 1–11, <https://doi.org/10.1029/2004PA001039>, 2004.
- Lear, C. H., Coxall, H. K., Foster, G. L., Lunt, D. J., Mawbey, E. M., Rosenthal, Y., Sosdian, S. M., Thomas, E., and Wilson, P. A.: Neogene ice volume and ocean temperatures: Insights from infaunal foraminiferal Mg/Ca paleothermometry, *Paleoceanography*, 30, 1437–1454, <https://doi.org/10.1002/2015PA002833>, 2015.
- LeGrande, A. N. and Schmidt, G. A.: Global gridded data set of the oxygen isotopic composition in seawater, *Geophys. Res. Lett.*, 33, 1–5, <https://doi.org/10.1029/2006GL026011>, 2006.
- Lisiecki, L. E. and Raymo, M. E.: A Pliocene-Pleistocene stack of 57 globally distributed benthic $\delta^{18}\text{O}$ records, *Paleoceanography*, 20, 1–17, <https://doi.org/10.1029/2004PA001071>, 2005.
- Lynch-Stieglitz, J., Curry, W. B., and Slowey, N.: A geostrophic transport estimate for the Florida Current from the oxygen isotope composition of benthic foraminifera, *Paleoceanography*, 14, 360–373, <https://doi.org/10.1029/1999PA900001>, 1999.
- Martin, P. A. and Lea, D. W.: A simple evaluation of cleaning procedures on fossil benthic foraminiferal Mg/Ca, *Geochem. Geophys. Geos.*, 3, 1–8, <https://doi.org/10.1029/2001GC000280>, 2002.
- M'Boule, D., Chivall, D., Sinke-Schoen, D., Sinninghe Damsté, J., Schouten, S., and van der Meer, M. T. J.: Salinity dependent hydrogen isotope fractionation in alkenones produced by coastal and open ocean haptophyte algae, *Geochim. Cosmochim. Acta*, 130, 126–135, <https://doi.org/10.1016/j.gca.2014.01.029>, 2014.
- McCrea, J. M.: On the Isotopic Chemistry of Carbonates and a Paleotemperature Scale, *J. Chem. Phys.*, 18, 849–857, <https://doi.org/10.1063/1.1747785>, 1950.
- Menschel, E., González, H. E., and Giesecke, R.: Coastal-oceanic distribution gradient of coccolithophores and their role in the carbonate flux of the upwelling system off Concepción, Chile (36° S), *J. Plankton Res.*, 38, 798–817, <https://doi.org/10.1093/plankt/fbw037>, 2016.
- Mitsunaga, B. A., Novak, J., Zhao, X., Dillon, J. A., Huang, Y., and Herbert, T. D.: Alkenone $\delta^2\text{H}$ values – a viable seawater isotope proxy? New core-top $\delta^2\text{HC}_{37:3}$ and $\delta^2\text{HC}_{37:2}$ data suggest inter-alkenone and alkenone-water hydrogen isotope fractionation are independent of temperature and salinity, *Geochim. Cosmochim. Acta*, 339, 139–156, <https://doi.org/10.1016/j.gca.2022.10.024>, 2022.
- Mix, A., Tiedemann, R., and Blum, P.: Proceedings of the Ocean Drilling Program, Vol. 202, Initial Reports, Southeast Pacific Paleooceanographic Transects, *Ocean Drill. Progr.*, <https://doi.org/10.2973/odp.proc.ir.202.2003>, 2003.
- Mulitza, S., Boltovskoy, D., Donner, B., Meggers, H., Paul, A., and Wefer, G.: Temperature: $\delta^{18}\text{O}$ relationships of planktonic foraminifera collected from surface waters, *Palaeogeogr. Palaeoclimatol. Palaeoecol.*, 202, 143–152, [https://doi.org/10.1016/S0031-0182\(03\)00633-3](https://doi.org/10.1016/S0031-0182(03)00633-3), 2003.
- Muratli, J. M., Chase, Z., Mix, A. C., and McManus, J.: Increased glacial-age ventilation of the Chilean margin by Antarctic Intermediate Water, *Nat. Geosci.*, 3, 23–26, <https://doi.org/10.1038/ngeo715>, 2010.
- Oba, T. and Murayama, M.: Sea-surface temperature and salinity changes in the northwest Pacific since the last glacial maximum, *J. Quaternary Sci.*, 19, 335–346, <https://doi.org/10.1002/jqs.843>, 2004.
- O'Neil, J. R., Clayton, R. N., and Mayeda, T. K.: Oxygen Isotope Fractionation in Divalent Metal Carbonates, *J. Chem. Phys.*, 51, 5547–5558, <https://doi.org/10.1063/1.1671982>, 1969.
- Pahnke, K., Sachs, J. P., Keigwin, L., Timmermann, A., and Xie, S. P.: Eastern tropical Pacific hydrologic changes during the past 27,000 years from D/H ratios in alkenones, *Paleoceanography*, 22, 1–15, <https://doi.org/10.1029/2007PA001468>, 2007.
- Pearson, P. N.: Oxygen Isotopes in Foraminifera: Overview and Historical Review, *Paleontol. Soc. Pap.*, 18, 1–38, <https://doi.org/10.1017/s1089332600002539>, 2012.
- Petersen, S. V. and Schrag, D. P.: Antarctic ice growth before and after the Eocene-Oligocene transition: New estimates

- from clumped isotope paleothermometry, *Paleoceanography*, 30, 1305–1317, <https://doi.org/10.1002/2014PA002769>, 2015.
- Petrick, B. F., McClymont, E. L., Marret, F., and Van Der Meer, M. T. J.: Changing surface water conditions for the last 500 ka in the Southeast Atlantic: Implications for variable influences of Agulhas leakage and Benguela upwelling, *Paleoceanography*, 30, 1153–1167, <https://doi.org/10.1002/2015PA002787>, 2015.
- Prahl, F. G. and Wakeham, S. G.: Calibration of unsaturation patterns in long-chain ketone compositions for palaeotemperature assessment, *Nature*, 330, 367–369, <https://doi.org/10.1038/330367a0>, 1987.
- Putman, A. L., Fiorella, R. P., Bowen, G. J., and Cai, Z.: A Global Perspective on Local Meteoric Water Lines: Meta-analytic Insight Into Fundamental Controls and Practical Constraints, *Water Resour. Res.*, 55, 6896–6910, <https://doi.org/10.1029/2019WR025181>, 2019.
- Rohling, E. J.: Progress in paleosalinity: Overview and presentation of a new approach, *Paleoceanography*, 22, 1–9, <https://doi.org/10.1029/2007PA001437>, 2007.
- Rohling, E. J. and Bigg, G. R.: Paleosalinity and $\delta^{18}\text{O}$: A critical assessment, *J. Geophys. Res.-Oceans*, 103, 1307–1318, <https://doi.org/10.1029/97jc01047>, 1998.
- Rohling, E. J. and Cooke, S.: Stable oxygen and carbon isotopes in foraminiferal carbonate shells, in: *Modern Foraminifera*, Springer Netherlands, Dordrecht, 239–258, https://doi.org/10.1007/0-306-48104-9_14, 1999.
- Rostek, F., Ruhlandt, G., Bassinot, F. C., Muller, P. J., Labeyrie, L. D., Lancelot, Y., and Bard, E.: Reconstructing sea surface temperature and salinity using $\delta^{18}\text{O}$ and alkenone records, *Nature*, 364, 319–321, <https://doi.org/10.1038/364319a0>, 1993.
- Rostek, F., Bard, E., Beaufort, L., Sonzogni, C., and Ganssen, G.: Sea surface temperature and productivity records for the last 240 kyr on the Arabian Sea, *Deep-Sea Res. Pt. II*, 44, 1461–1480, [https://doi.org/10.1016/S0967-0645\(97\)00008-8](https://doi.org/10.1016/S0967-0645(97)00008-8), 1997.
- Rousselle, G., Beltran, C., Sicre, M. A., Raffi, I., and De Rafélis, M.: Changes in sea-surface conditions in the Equatorial Pacific during the middle Miocene-Pliocene as inferred from coccolith geochemistry, *Earth Planet. Sc. Lett.*, 361, 412–421, <https://doi.org/10.1016/j.epsl.2012.11.003>, 2013.
- Sachs, J. P. and Kawka, O. E.: The influence of growth rate on $^2\text{H}/^1\text{H}$ fractionation in continuous cultures of the coccolithophorid *Emiliana huxleyi* and the diatom *Thalassiosira pseudonana*, *PLoS One*, 10, 1–27, <https://doi.org/10.1371/journal.pone.0141643>, 2015.
- Sachs, J. P., Maloney, A. E., Gregersen, J., and Paschall, C.: Effect of salinity on $^2\text{H}/^1\text{H}$ fractionation in lipids from continuous cultures of the coccolithophorid *Emiliana huxleyi*, *Geochim. Cosmochim. Ac.*, 189, 96–109, <https://doi.org/10.1016/j.gca.2016.05.041>, 2016.
- Schouten, S., Hopmans, E. C., Schefuß, E., and Sinninghe Damsté, J. S.: Corrigendum to “Distributional variations in marine crenarchaeotal membrane lipids: a new tool for reconstructing ancient sea water temperatures?”, *Earth Planet. Sc. Lett.*, 211, 205–206, [https://doi.org/10.1016/S0012-821X\(03\)00193-6](https://doi.org/10.1016/S0012-821X(03)00193-6), 2003.
- Schouten, S., Ossebaar, J., Schreiber, K., Kienhuis, M. V. M., Langer, G., Benthien, A., and Bijma, J.: The effect of temperature, salinity and growth rate on the stable hydrogen isotopic composition of long chain alkenones produced by *Emiliana huxleyi* and *Gephyrocapsa oceanica*, *Biogeosciences*, 3, 113–119, <https://doi.org/10.5194/bg-3-113-2006>, 2006.
- Schrag, D. P., Adkins, J. F., McIntyre, K., Alexander, J. L., Hodell, D. A., Charles, C. D., and McManus, J. F.: The oxygen isotopic composition of seawater during the Last Glacial Maximum, *Quaternary Sci. Rev.*, 21, 331–342, [https://doi.org/10.1016/S0277-3791\(01\)00110-X](https://doi.org/10.1016/S0277-3791(01)00110-X), 2002.
- Shackleton, N. J.: Attainment of isotopic equilibrium between ocean water and the benthonic foraminifera genus *Uvigerina*: Isotopic changes in the ocean during the last glacial, *Colloq. Int. du C.N.R.S.*, 219, 203–210, 1974.
- Simon, M. H., Gong, X., Hall, I. R., Ziegler, M., Barker, S., Knorr, G., Van Der Meer, M. T. J., Kasper, S., and Schouten, S.: Salt exchange in the Indian-Atlantic Ocean Gateway since the Last Glacial Maximum: A compensating effect between Agulhas Current changes and salinity variations?, *Paleoceanography*, 30, 1318–1327, <https://doi.org/10.1002/2015PA002842>, 2015.
- Spero, H. J., Bijma, J., Lea, D. W., and Bemis, B. E.: Effect of seawater carbonate concentration on foraminiferal carbon and oxygen isotopes, *Lett. Nat.*, 390, 497–500, 1997.
- Spero, H. J., Mielke, K. M., Kalve, E. M., Lea, D. W., and Pak, D. K.: Multispecies approach to reconstructing eastern equatorial Pacific thermocline hydrography during the past 360 kyr, *Paleoceanography*, 18, 1–16, <https://doi.org/10.1029/2002PA000814>, 2003.
- Srivastava, R., Ramesh, R., Jani, R. A., Anilkumar, N., and Sudhakar, M.: Stable oxygen, hydrogen isotope ratios and salinity variations of the surface Southern Indian Ocean waters, *Curr. Sci.*, 99, 1395–1399, 2010.
- Strub, P. T., Mesías, M. J., Montecino, V., Rutllant, J., and Salinas, S.: Coastal ocean circulation off western South America coastal segment, in: *The Sea*, vol. 11, John Wiley & Sons, 273–313, ISBN 0-471-11545-2, 1998.
- Tang, C. M. and Stott, L. D.: Seasonal salinity changes during Mediterranean sapropel deposition 9000 years B.P.: Evidence from isotopic analyses of individual planktonic foraminifera, *Paleoceanography*, 8, 473–493, <https://doi.org/10.1029/93PA01319>, 1993.
- Van der Meer, M. T. J., Benthien, A., Bijma, J., Schouten, S., and Sinninghe Damsté, J. S.: Alkenone distribution impacts the hydrogen isotopic composition of the $\text{C}_{37:2}$ and $\text{C}_{37:3}$ alkan-2-ones in *emiliana huxleyi*, *Geochim. Cosmochim. Ac.*, 111, 162–166, <https://doi.org/10.1016/j.gca.2012.10.041>, 2013.
- van der Meer, M. T. J., Benthien, A., French, K. L., Epping, E., Zondervan, I., Reichart, G. J., Bijma, J., Sinninghe Damsté, J. S., and Schouten, S.: Large effect of irradiance on hydrogen isotope fractionation of alkenones in *Emiliana huxleyi*, *Geochim. Cosmochim. Ac.*, 160, 16–24, <https://doi.org/10.1016/j.gca.2015.03.024>, 2015.
- Varma, D., Hättig, K., van der Meer, M. T. J., Reichart, G.-J., and Schouten, S.: SST Proxies Chilean (ODP Leg 202 Site 1235 and Site 1234) and Angola Margin (ODP Leg 175 Site 1078 and Site 1079), PANGAEA [data set], <https://doi.org/10.1594/PANGAEA.957090>, 2023a.
- Varma, D., Hättig, K., van der Meer, M. T. J., Reichart, G.-J., and Schouten, S.: Constraining Water Depth Influence on Organic Paleotemperature Proxies using Sedimentary Archives, *Paleoceanogr. Paleoclim.*, 38, e2022PA004533, <https://doi.org/10.1029/2022PA004533>, 2023b.

- Waelbroeck, C., Labeyrie, L., Michel, E., Duplessy, J. C., McManus, J. F., Lambeck, K., Balbon, E., and Labracherie, M.: Sea-level and deep water temperature changes derived from benthic foraminifera isotopic records, *Quaternary Sci. Rev.*, 21, 295–305, [https://doi.org/10.1016/S0277-3791\(01\)00101-9](https://doi.org/10.1016/S0277-3791(01)00101-9), 2002.
- Weiss, G. M., Pfannerstill, Y. E., Schouten, S., Sinninghe Damsté, S. J., and van der Meer, T. J. M.: Effects of alkalinity and salinity at low and high light intensity on hydrogen isotope fractionation of long-chain alkenones produced by *Emiliania huxleyi*, *Biogeosciences*, 14, 5693–5704, <https://doi.org/10.5194/bg-14-5693-2017>, 2017.
- Weiss, G. M., Schouten, S., Sinninghe Damsté, J. S., and van der Meer, M. T. J.: Constraining the application of hydrogen isotopic composition of alkenones as a salinity proxy using marine surface sediments, *Geochim. Cosmochim. Ac.*, 250, 34–48, <https://doi.org/10.1016/j.gca.2019.01.038>, 2019a.
- Weiss, G. M., de Bar, M. W., Stolwijk, D. J., Schouten, S., Sinninghe Damsté, J. S., and van der Meer, M. T. J.: Paleosensitivity of Hydrogen Isotope Ratios of Long-Chain Alkenones to Salinity Changes at the Chile Margin, *Paleoceanogr. Paleocl.*, 34, 978–989, <https://doi.org/10.1029/2019PA003591>, 2019b.
- Zhang, X., Gillespie, A. L., and Sessions, A. L.: Large D/H variations in bacterial lipids reflect central metabolic pathways, *P. Natl. Acad. Sci. USA*, 106, 12580–12586, <https://doi.org/10.1073/pnas.0903030106>, 2009.
- Zhang, Z. and Sachs, J. P.: Hydrogen isotope fractionation in freshwater algae: I. Variations among lipids and species, *Org. Geochem.*, 38, 582–608, <https://doi.org/10.1016/j.orggeochem.2006.12.004>, 2007.
- Zweng, M. M., Reagan, J. R., Seidov, D., Boyer, T. P., Locarnini, R. A., Garcia, H. E., Mishonov, A. V., Baranova, O. K., Weathers, K., Paver, C. R., and Smolyar, I.: World Ocean Atlas 2018, in: Vol. 2: Salinity, edited by: Mishonov, A., NOAA Atlas NESDIS 82, 50 pp., <https://www.ncei.noaa.gov/products/world-ocean-atlas> (last access: 11 October 2023), 2018.